BIOLOGY, MEDICINE, & NATURAL PRODUCT CHEMISTRY ISSN 2089-6514 (paper)
Volume 15, Number 1, April 2026 | Pages: 1-14 | DOI: 10.14421/biomedich.2026.151.1-14 ISSN 2540-9328 (online)

Antioxidant Activity Test of Ethanol Extract and Seburo Leaf Fraction (*Garcinia forbesii* King) in Male Wistar Rats Induced by CCl_4

Salni[1]*, Vitri Agustiarini[2], Gina Nurhasana[2]
[1]Department of Biology; [2]Department of Pharmacy, Faculty of Mathematics and Natural Sciences, Sriwijaya University, Ogan Ilir 30662, Indonesia.

Corresponding author*
salnibasir@unsri.ac.id

Manuscript received: 22 October, 2025. Revision accepted: 15 December, 2025. Published: 01 April, 2026.

Abstract

Seburo (*Garcinia forbesii* King) leaves have long been used in traditional medicine in Eastern Indonesia. Previous *in vitro* studies have demonstrated their significant antioxidant potential. This study aimed to characterize the phytochemical composition and evaluate the *in vivo* antioxidant activity of ethanol extracts and solvent fractions of *Seburo* leaves using a CCl_4-induced hepatotoxicity model in male Wistar rats. Antioxidant efficacy was assessed through measurements of malondialdehyde (MDA) levels, catalase enzyme activity, and both macroscopic and histopathological evaluation of liver tissue. Rats were divided into six groups: negative control (1% Na-CMC), positive control (vitamin C, 10 mg/kg BW), and four treatment groups receiving ethanol extract, n-hexane fraction, ethyl acetate fraction, and ethanol-water fraction (each at 100 mg/kg BW). The n-hexane fraction exhibited the strongest antioxidant activity, with significantly lower MDA levels (0.748 ± 0.061 nmol/mL) and higher catalase activity (27.694 ± 1.135 U/mL), comparable to the positive control. Liver examination revealed reduced tissue damage in all treatment groups compared to the negative control. GC-MS analysis identified key terpenoid compounds in ethanol extract, namely, lupeol, α-copaene, phytol, and friedelan-3-one, likely contributing to the antioxidant activity. N-hexane fraction has the most significant antioxidant activity among fractions, presumably as it contains the most diverse phytochemical profile. These findings support the therapeutic potential of *Seburo* leaf as a natural antioxidant agent.

Keywords: Catalase; CCl4; *Garcinia forbesii* King; liver histopathology; MDA.

INTRODUCTION

Antioxidants can mitigate and avert damage induced by reactive oxygen species (ROS) and reactive nitrogen species (RNS) (Flieger et al., 2021). Antioxidants function as scavengers, inhibiting tissue damage. The preventative process, healing mechanisms, and physical defense provided by antioxidants assist cells in combating excess free radicals (To et al., 2020). However, the consumption of synthetic antioxidants may induce adverse health effects, hence restricting their utilization. Kornienko et al (2019) shown that the consumption of elevated amounts of synthetic antioxidants may result in DNA damage and accelerated ageing. These issues have favorably impacted on the ongoing search for natural antioxidants derived from plants.

One of the plants with antioxidant properties is from the Clusiaceae family, namely *seburo* (*Garcinia forbesii King*). Wairata et al (2022) empirically demonstrate that *seburo* has been utilized in eastern Indonesia as a traditional remedy for malaria and diabetes. *Seburo* leaf are positively identified to include alkaloids, steroids, tannins, flavonoids, and phenols (Sutomo et al., 2020). Additionally, *seburo* leaf contain xanthones which were assessed for their antioxidant activities using in vitro assays, revealing promising results and solidifying the role of these compounds in the antioxidant effects observed in the extracts (Wairata et al., 2021). The ethanol extracts exhibit substantial antioxidant activity, as assessed by the DPPH technique, with an IC_{50} value of 534.69 ppm (Muthia et al., 2019). Another investigation indicated that methanolic extracts of the leaves exhibited antioxidant activity, as reflected by IC_{50} of 1.05% in DPPH assays (Haris & Sani, 2022).

Thus, further investigation into the in vivo antioxidant activity of the seburo leaf is imperative. This study will evaluate the antioxidant potential of both the *seburo* leaf extract and its fraction in male Wistar rats induced with CCl_4. The antioxidant capabilities will be assessed through both biochemical markers and physical evaluations of liver organ. Specifically, biomarkers such as malondialdehyde (MDA) levels and catalase enzyme activity will be measured, while physical assessments will involve macroscopic observation and histopathological examination of liver tissue. The investigation also characterizes the potential phytochemical compounds present in the extract and fractions using quantitative and qualitative assessments.

MATERIALS AND METHODS

Chemical and reagents

The research utilized several chemical reagents, including: 96% ethanol (PT. Bratachem, Palembang), n-hexane (PT. Bratachem, Palembang), ethyl acetate (PT. Bratachem, Palembang), distilled water, olive oil (Organic®), carbon tetrachloride (CCl4) (Sigma Aldrich® , Singapore), vitamin C (Merck KGgA® , Germany), 20% Trichloroacetic Acid (TCA) (Merck KGgA®, Germany), 1,1,3,3-tetraethoxypropane (TEP) (Sigma Aldrich® , Singapore), 0.67% thiobarbituric acid (TBA) (Sigma Aldrich® , Singapore), 0.9% physiological NaCl, 1% sodium carboxyl methyl cellulose (Na-CMC), sodium agar, magnesium powder, 1% $FeCl_3$, Hematoxylin-Eosin dye, 1 M sodium acetate, 10% $AlCl_3$, 10% sodium hydroxide, chloroform, acetic anhydride, concentrated hydrochloric acid, concentrated sulfuric acid, Mayer's reagent, Dragendorf reagent, Liebermann-Burchard reagent, Wagner reagent, filter paper (Whatman®, South Jakarta), aluminum foil, quercetin, acetic acid, Folin Ciocalteau reagent, sodium carbonate, and gallic acid.

Seburo leaf procurement

Seburo leaves (*Garcinia forbesii* King) were collected from mature plants in Tanjung Batu, Ogan Ilir District, South Sumatra Province, Indonesia. The site was chosen to minimize exposure to environmental contaminants. Only healthy, undamaged leaves were selected, washed to remove debris, and shade-dried at room temperature to preserve active compounds. Dried leaves were stored in airtight, light-resistant containers under cool, dry conditions before extraction.

Extraction and fractionation of *seburo* leaf

Seburo leaf was washed thoroughly, dried in indirect sunlight, and covered with black cloth. The leaves were processed in a blender until a fine powder is achieved. 1000 g of *seburo* leaf were macerated in six liters of 96% ethanol for three days, followed by filtration. This process was repeated twice, with an additional two days of maceration using four liters of 96% ethanol, and subsequent filtration. The filtrate was subsequently concentrated using a rotary evaporator at a maximum temperature of 60 °C.

Fractionation was performed via the liquid-liquid partition technique with n-hexane, ethyl acetate, and ethanol-water solvents. The concentrated ethanol extract of *seburo* leaf was subsequently fractionated in succession using n-hexane, ethyl acetate, and ethanol-water solvents. The concentrated extract of *seburo* leaf was dissolved in a 1:1 ethanol-water solvent, followed by the addition of 200 mL of n-hexane. The resulting mixture was agitated and allowed to stand until the boundary between the two solvents became apparent. Subsequently, the n-hexane fraction and the ethanol-water fraction were separated and removed from the separating funnel. The residual ethanol-water combination was combined with 200 mL ethyl acetate solution, followed by agitation and allowing it to rest until a boundary between the two solvents became apparent. Subsequent to separation, the ethyl acetate fraction and the ethanol-water fraction were extracted from the separating funnel. The fractionation outcomes of each solvent were concentrated using a rotary evaporator at 60°C to get a viscous n-hexane fraction, a viscous ethyl acetate fraction, and a viscous ethanol-water fraction.

Determination of total flavonoid content

The determination of total flavonoid content (TFC) using UV-Vis spectrophotometry typically employs a colorimetric method that involves aluminum chloride ($AlCl_3$) as the reagent (Wathan et al., 2023; Widiyana & Illian, 2022). Quercetin was used as the standard. A stock solution of 1000 ppm was prepared by dissolving 10 mg of quercetin in 10 mL of methanol. From this, a 40-ppm working solution was obtained by diluting 4 mL of the stock solution to 100 mL with methanol p.a. Serial dilutions of 20, 24, 28, 32, and 36 ppm were prepared by pipetting 5, 6, 7, 8, and 9 mL of the 40-ppm solution, respectively. Each standard solution (3 mL) was mixed with 0.2 mL of 10% $AlCl_3$ and 0.2 mL of 1 M sodium acetate, then diluted to 10 mL with distilled water. After 30 minutes of incubation at room temperature, absorbance was measured at 435 nm using a UV-Vis spectrophotometer. The calibration curve was plotted using quercetin concentration (ppm) versus absorbance.

For sample analysis, 10 mg of each extract or fraction was dissolved in 10 mL of ethanol p.a. to obtain a 1000 ppm solution. From this, 3 mL was treated with 0.2 mL of 10% $AlCl_3$ and 0.2 mL of 1 M sodium acetate, then brought to 10 mL with distilled water. After a 30-minute incubation at ambient temperature, absorbance was measured at 435 nm. All samples were analyzed in triplicate, and the average absorbance values were used to calculate the flavonoid content based on the standard curve.

Determination of total phenolic content

The total phenolic content (TPC) was determined using the Folin-Ciocalteu colorimetric method, which quantifies phenolic compounds based on their ability to reduce the Folin-Ciocalteu reagent, forming a blue chromophore measured spectrophotometrically at 765–766 nm (Aswar et al., 2021; Wulandari et al., 2020). Gallic acid was used as the standard. A 1000 ppm stock solution was prepared by dissolving 10 mg of gallic acid in 10 mL of methanol. From this, a 400-ppm working solution was obtained by diluting 4 mL of the stock with methanol to a final volume of 10 mL. To determine the maximum absorbance wavelength, 0.5 mL of the 400-ppm solution was mixed with 1 mL of Folin-Ciocalteu reagent and allowed to stand for 5 minutes. Then, 2 mL

of 15% Na_2CO_3 solution was added, and the volume was adjusted to 10 mL with distilled water. The absorbance spectrum was recorded in the range of 500–900 nm to identify the maximum wavelength, which was found to be 765 nm.

For the calibration curve, gallic acid solutions of 100, 150, 200, 250, and 300 ppm were prepared. For each concentration, 0.5 mL was reacted with 1 mL of Folin-Ciocalteu reagent, incubated for 5 minutes, followed by the addition of 2 mL of 15% Na_2CO_3 solution. The volume was adjusted to 10 mL with distilled water and left to stand for 30 minutes at room temperature. Absorbance was measured at 765 nm, and a standard curve was plotted using concentration versus absorbance. Linear regression analysis was used to derive the correlation coefficient.

For sample analysis, 100 mg of extract or fraction was dissolved in 100 mL of methanol p.a. to yield a 1000 ppm solution. A 10 mL aliquot was then diluted to 100 mL to obtain a 100-ppm solution. From this, 1 mL was mixed with 1 mL of Folin-Ciocalteu reagent and incubated for 5 minutes. Then, 2 mL of 15% Na_2CO_3 solution was added, and the volume was adjusted to 10 mL with distilled water. After incubation for 30 minutes at room temperature, absorbance was recorded at 765 nm. All measurements were performed in triplicate, and the total phenolic content was expressed as mg gallic acid equivalents (GAE) per gram of sample based on the standard curve.

Determination of antioxidant compound classes

The identification of antioxidant compound classes in seburo leaf ethanol extract and its fractions was performed using the thin layer chromatography (TLC) method. Each sample was spotted onto silica gel plates and developed using an appropriate solvent system. After development, the plates were sprayed with 0.008% DPPH solution to detect antioxidant-active compounds, indicated by the appearance of yellow spots on a purple background. To further visualize compound classes, the plates were also sprayed with 1% H_2SO_4 and heated to enhance color differentiation. Observations of color changes allowed for the presumptive identification of various phytochemical groups contributing to antioxidant activity. The R_f (retardation factor) values were calculated by dividing the distance traveled by each compound by the distance traveled by the solvent front. R_f values are used to compare the mobility and potential identity of active constituents across different fractions.

Determinations of antioxidant compound

Identification of possible antioxidant compounds was conducted using gas chromatography mass spectrometry (GC-MS) utilizing a Thermo Scientific Trace 1310 gas chromatograph and a Thermo Scientific ISQLT single quadrupole mass spectrometer, both fitted with a 30 m long, 0.25 mm diameter, and 0.25 µm film thickness fused silica capillary column HP-5MS UI. The column oven temperature was set to increase from 60 °C to 280 °C at a rate of 10 °C/min during a duration of 8 minutes. The ionization of sample components was performed using electron impact mode (EI, 70 eV). The injector temperature was established at 230 °C. The carrier gas employed was ultra-high-purity helium (He) (99.99%) with a flow rate of 1 mL/min, scanning a mass range of 40–500 m/z at a rate of 3 scans per second. The paste sample was dissolved in 1.5 mL of MeOH in a microtube, then vortexed until homogeneous; if necessary, it was centrifuged at 9500 rpm for 3 minutes. The supernatant was transferred to a GC vial, and the sample solution was prepared for injection. The overall duration for GC-MS was 32 minutes. The GC retention time determined the identification and characterization of chemical components in the extract. Computer analysis calibrated the mass spectrum using standards from the mass spectrum library.

Animal experimentation

CCl_4-induced hepatotoxicity model

A total of 26 male Wistar rats was required, with 4 rats allocated to each group. Each group was supplemented by one mouse to prevent sample deficiencies, resulting in a total requirement of 30 rats. The test subjects are randomly selected and allocated into six treatment groups. Each animal group received various solution orally, as illustrated in **Table 1**. The parameters evaluated in this study include MDA levels, catalase enzyme activity, macroscopic characteristics, and hepatological characteristics.

Table 1. Experimental group design and treatment regimen.

Groups	Treatment
Positive	Vitamin C 10 mg/kgBW + CCl_4 1 mL/kgBW
Negative	Na CMC 1% suspension+ CCl_4 1 mL/kgBW
Test Group I	100 mg/kgBW ethanol extract + CCl_4 1 mL/kgBW
Test Group II	100 mg/kgBW n-hexane fraction + CCl_4 1 mL/kgBW
Test Group III	100 mg/kgBW ethyl acetate fraction + CCl_4 1 mL/kgBW
Test Group IV	100 mg/kgBW ethanol-water fraction + CCl_4 1 mL/kgBW

MDA level assessment

The procedure for measuring MDA levels employs the thiobarbituric acid (TBA) assay. This method is well-established for assessing MDA concentrations as a reflection of oxidative stress (Tsikas, 2017). MDA levels were assessed on day 8 after treatment from day 1 to day 6, as outlined in Table 1. Blood was collected from the medial canthus of the orbital sinus of each test animal following an 8-hour fasting period. Approximately ± 2 mL of blood was collected and preserved in an EDTA vacutainer tube. MDA levels were quantified by incubating 2 mL of blood samples at 37°C for 15 minutes, followed by centrifugation at 3000 rpm for 5 minutes to separate the plasma from the blood cells of the rats. 1 mL of supernatant was combined with 0.5 mL of 20% trichloroacetic acid (TCA) and subsequently centrifuged at 3000 rpm for 5 minutes to get protein-free blood plasma. The supernatant was taken as much as 1 mL, then put into a test tube and added with 1 mL of 0.67% TBA solution, shaken until homogeneous. The test tube was subjected to heating in a water bath at a temperature of 95-100 °C for the duration established from the assessment of the operational time following the cooling of the solution with running water or an ice bath. The resultant pink solution was subsequently assessed for its absorbance at a wavelength derived from the protocol for ascertaining the wavelength of the TEP standard solution. The MDA content was quantified using the TEP standard curve regression equation, with the X-axis representing MDA content and the Y-axis denoting absorbance values.

Catalase enzyme activity assessment

The assessment of catalase enzyme activity was conducted utilizing spectrophotometric techniques on tissue homogenates in response to H_2O_2. The test subjects were euthanized via cervical dislocation, followed by surgical excision of the liver. The liver specimen was sectioned and promptly rinsed with ice-cold saline to eliminate blood. A 10% w/v homogenate was made in cold 0.05 M phosphate buffer (pH 7) and subsequently centrifuged at 1000 rpm at 4°C for 10 minutes. The transparent supernatant obtained from centrifugation was utilized to assess catalase enzyme activity. 1 mL of liver homogenate was combined with 5 mL of 50 mM phosphate buffer (pH 7) and subjected to stirring. Subsequently, 4 mL of 0.2 M H_2O_2 was introduced and allowed to incubate for 30 seconds. This solution is referred to as the test solution. A standard solution consists of H_2O_2 with concentrations of 0.04, 0.08, 0.12, 0.16, 0.2, and 0.4 M. Subsequently, 1 mL of the test solution is transferred into a test tube and combined with 2 mL of 5% $K_2Cr_2O_7$. The tube is subjected to boiling water for a duration of 10 minutes. Upon cooling, the absorbance of the test solution is measured at a wavelength of 570-610 nm. The absorbance measurement corresponds to the concentration of the residual H_2O_2. The quantity of H_2O_2 utilized by catalase is 0.2 M subtracted by the measured concentration of H_2O_2. One unit of catalase activity is defined as the quantity of H_2O_2 in moles consumed by catalase per minute.

Macroscopic observation and histological examination of liver

A macroscopic observation of the liver was performed by assessing organ weight and surface morphology. This was followed by histological analysis to evaluate tissue-level changes. Liver histology from each treatment group was examined for structural alterations in hepatocytes, including signs of hydropic degeneration, fatty degeneration (steatosis), and necrosis (Desmawati et al., 2022; Rahma & Purnomo, 2023). The extent of liver damage was assessed using the Manja Roenigk scoring system scoring criteria detailed in **Table 2**, **Table 3**, and **Table 4** (Purkon et al., 2022; Zega et al., 2023).

Table 2. Hydropic degeneration scoring parameters.

Score	Hepatological characteristics
0	< 25% of liver exhibits hydropic degeneration, parenchymal degeneration and apoptosis around the centrilobular (central vein)
1	25-50% of liver exhibits hydropic degeneration, parenchymal degeneration and apoptosis that extend to the central area (midzone)
2	50-75% of liver exhibits hydropic degeneration, parenchymal degeneration and apoptosis that extends to the periportal (perilobular)
3	>75% of liver exhibits hydropic degeneration, parenchymal degeneration and apoptosis extending to the periportal (perilobular)

Table 3. Fatty degeneration scoring parameters.

Score	Fatty Degeneration (Steatosis) Criteria
0	Normal
1	Mild (< 10% of hepatocytes exhibit steatosis)
2	Moderate (10-30% of hepatocytes exhibit steatosis)
3	Severe (> 30% of hepatocytes exhibit steatosis)

Tabel 4. Necrosis scoring parameters.

Score	Necrotic Degeneration Criteria
0	Normal
1	Mild (< 10% hepatocytes exhibit necrosis)
2	Moderate (10-30% hepatocytes exhibit necrosis)
3	Severe (> 30% hepatocytes exhibit necrosis)
4	Massive necrosis

RESULTS AND DISCUSSION

Result

Extraction and fractionation yield

The thick extract yielded 182.68 grams from 1000 grams of simplicial powder, resulting in a percentage yield of 18.268%. The results comply with the quality standards for the yield of medicinal plants, namely exceeding 11% (Departemen Kesehatan RI, 2000). The percentage yield achieved was approximately consistent with the findings of (Sutomo et al., 2021) which reported 204.04 grams (20.404%) from 1500 grams of extracted simplicia. The variance in yield values is affected by multiple factors, including the quantity of simplicia, the solvent type, the size of the simplicia, the duration of maceration, and the polarity of the solvent (Hidayati et al., 2017)

Table 5. Fraction weight and percentage yield of seburo leaf fraction.

Fraction	Fraction weight (g)	Percentage yield (%)
N-hexane	7.34	5.35
Ethyl acetate	56.15	40.98
Ethanol-water	73.52	53.66

Total flavonoid content

Total flavonoid content of the extract is expressed in the form of QE and is shown in **Table 6**. TFC was calculated using the following linear regression equation obtained from the standard quercetin plot: y = 0.0279x – 0.3579 with a correlation value (R^2) of 0.9994. Where y is the absorption and x is the amount of quercetin equivalent.

Table 6. Total flavonoid content of seburo leaf extract and its fractions.

Sample	Total Flavonoid Content (mg QE/g)	Percentage (%)
Ethanol extract	33.640 ± 0.744	3.364
N-hexane fraction	21.612 ± 0.245	2.161
Ethyl acetate fraction	32.165 ± 0.551	3.217
Ethanol-water fraction	19.989 ± 0.426	1.999

Total phenolic content

Total phenolic content of the extract is given in the form of GAE and is shown in **Table 7**. TPC was estimated using a linear regression equation developed from the standard plot of gallic acid: y = 0.0017x + 0.0446 with a correlation value (R^2) of 0.9996. Where y is the absorbance and x are the quantity of gallic acid.

Table 7. Results of calculating the total phenolic content of seburo leaf extract and fractions.

Sample	Total Phenolic Content (mg GAE/g)	Percentage (%)
Ethanol extract	76.376 ± 2.433	7.638
N-hexane fraction	51.692 ± 2.942	5.169
Ethyl acetate fraction	42.558 ± 3.315	4.256
Ethanol-water fraction	22.133 ± 3.062	2.213

Antioxidant compound of seburo leaves

The results of TLC analysis for the ethanol extract and its fractions are presented in **Table 8**. All samples exhibited antioxidant activity, as indicated by the appearance of yellow spots following treatment with 0.008% DPPH, which signifies free radical scavenging.

Table 8. TLC results of ethanol extract and seburo leaf fractions.

Sample	Rf (cm)	Stain Color	Compound Class	Antioxidant Activity
Ethanol extract	0.88	Orange yellow	Triterpenoid	++
	0.82	Bluish green	Steroid	++
	0.75	Yellow	Phenolic	+++
	0.57	Purple	Triterpenoid	++
	0.48	Yellow	Flavonoid	+++
	0.06	Brown	Tanin	+++
N-hexane fraction	0.93	Orange yellow	Triterpenoid	+++
	0.88	Bluish green	Steroid	+++
	0.71	Yellow	Phenolic	+++
	0.51	Purple	Triterpenoid	+++
	0.37	Yellow	Flavonoid	++
Ethly acetate fraction	0.73	Yellow	Phenolic	++
	0.44	Purple	Triterpenoid	+++
	0.42	Yellow	Flavonoid	+++
	0.06	Brown	Tanin	+++
Ethanol-water fraction	0.06	Brown	Tanin	+++

Remarks: Medium (++) and Strong (+++) [31]

GCMS analysis was employed for the identification and quantification of components in the ethanol extract of seburo leaves. Compounds were identified by analyzing molecular formula, retention time, molecular weight, and peak area. The findings of the GCMS investigation are presented in **Table 9** and **Figure 1**. The GCMS analysis found a total of 40 chemicals. The main compounds identified based on their relative contents were lupeol (34.16%), friedelan-3-one (14.04%), ethyl iso-allocholate (9.94%), dl-a-tocopherol (8.45%), phytol (8.13%), 11-octadecenoic acid, methyl ester (3.48%), alpha-copaene (3.42%), and hexadecanoic acid and methyl ester (2.03%) (**Table 10).**

Table 9. Phytochemical compounds identified in ethanol extract of seburo leaf using GC-MS.

No.	Retention time (min)	Compound	Molecular formula	Molecular weight	Peak Area (%)
1	10.44	alpha-Copaene	$C_{15}H_{24}$	204	3.42
2	11.03	Bicyclo[7.2.0]undec-4-ene, 4,11,11-trimethyl-8-methylene-,[1R-(1R*,4Z,9S*)]-	$C_{15}H_{24}$	204	0.92
3	11.47	7-epi-trans-sesquisabinene hydrate	$C_{15}H_{26}O$	222	0.14
4	11.75	7-epi-cis-sesquisabinene hydrate	$C_{15}H_{26}O$	222	0.19
5	12.33	ß-copaene	$C_{15}H_{24}$	204	0.24
6	13.08	Ethyl iso-allocholate	$C_{26}H_{44}O_5$	436	0.13
7	15.50	Ethyl iso-allocholate	$C_{26}H_{44}O_5$	436	0.12
8	15.81	Ethanol, 2-(9-octadecenyloxy)-, (Z)-	$C_{26}H_{44}O_5$	312	0.71
9	16.06	Ethyl iso-allocholate	$C_{26}H_{44}O_5$	436	0.12
10	16.24	Ethyl iso-allocholate	$C_{26}H_{44}O_5$	436	0.14
11	16.71	Hexadecanoic acid, methyl ester	$C_{17}H_{34}O_2$	270	2.03
12	18.36	11-Octadecenoic acid, methyl ester	$C_{19}H_{36}O_2$	296	3.48
13	18.59	Phytol	$C_{20}H_{40}O$	296	8.13
14	18.96	Ethyl iso-allocholate	$C_{26}H_{44}O_5$	436	0.16
15	19.17	Ethyl iso-allocholate	$C_{26}H_{44}O_5$	436	0.22
16	19.76	Ethyl iso-allocholate	$C_{26}H_{44}O_5$	436	0.23
17	20.20	Ethyl iso-allocholate	$C_{26}H_{44}O_5$	436	0.19
18	21.17	Ethyl iso-allocholate	$C_{26}H_{44}O_5$	436	0.16
19	21.40	Ethyl iso-allocholate	$C_{26}H_{44}O_5$	436	0.14
20	21.60	Ethyl iso-allocholate	$C_{26}H_{44}O_5$	436	0.12
21	22.11	3',8,8'-Trimethoxy-3-piperidyl-2,2'-binaphthalene-1,1',4,4'-tetrone	$C_{28}H_{25}NO_7$	487	0.86
22	22.64	Friedelan-3-one	$C_{30}H_{50}O$	426	14.04
23	23.96	Ethyl iso-allocholate	$C_{26}H_{44}O5$	436	0.14
24	24.13	2,2,4-Trimethyl-3-(3,8,12,16-tetramethyl-heptadeca-3,7,11,15-tetraenyl)-cyclohexanol	$C_{30}H_{52}O$	428	2.78
25	24.37	Ethyl iso-allocholate	$C_{26}H_{44}O_5$	436	0.56
26	24.53	Ethyl iso-allocholate	$C_{26}H_{44}O_5$	436	0.43
27	24.97	Ethyl iso-allocholate	$C_{26}H_{44}O_5$	436	0.12
28	25.42	Ethyl iso-allocholate	$C_{26}H_{44}O_5$	436	0.13
29	26.22	Ethyl iso-allocholate	$C_{26}H_{44}O_5$	436	0.80
30	26.37	Ethyl iso-allocholate	$C_{26}H_{44}O_5$	436	0.73
31	27.07	dl-a-Tocopherol	$C_{29}H_{50}O_2$	430	8.45
32	27.63	Ethyl iso-allocholate	$C_{26}H_{44}O_5$	436	0.97
33	28.98	Ethyl iso-allocholate	$C_{26}H_{44}O_5$	436	1.03
34	29.28	Ethyl iso-allocholate	$C_{26}H_{44}O_5$	436	0.19
35	30.08	Ethyl iso-allocholate	$C_{26}H_{44}O_5$	436	9.94
36	30.32	Ethyl iso-allocholate	$C_{26}H_{44}O_5$	436	0.02
37	30.37	Ethyl iso-allocholate	$C_{26}H_{44}O_5$	436	1.74
38	30.50	Ethyl iso-allocholate	$C_{26}H_{44}O_5$	436	1.04
39	30.89	Ethyl iso-allocholate	$C_{26}H_{44}O_5$	436	0.85
40	31.20	Lupeol	$C_{30}H_{50}O$	426	34.16

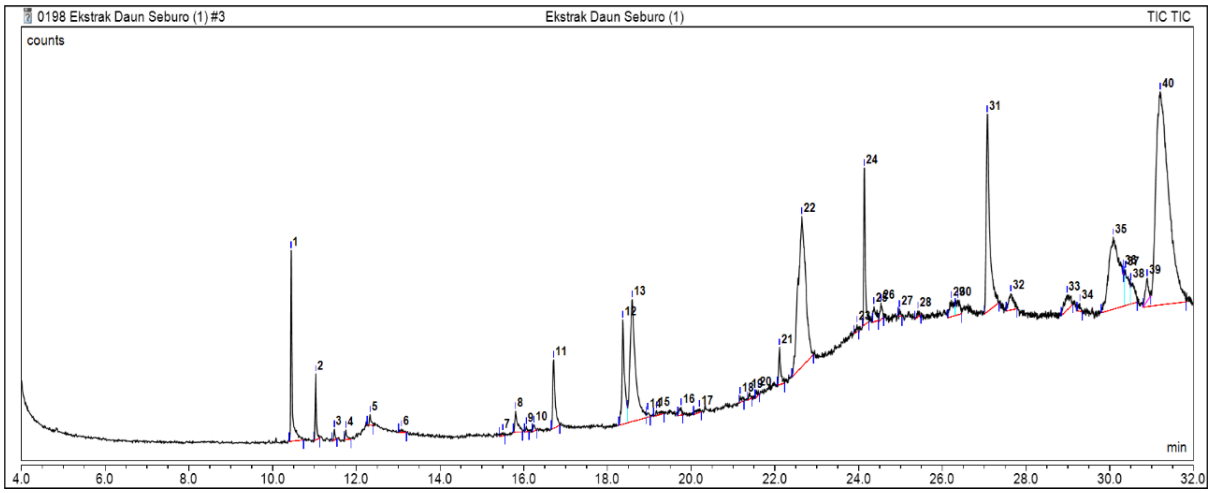

Figure 1. The result of GC-MS of seburo leaf ethanolic extract.

Table 10. Main compounds and their bioactive capabilities in ethanol extract of seburo leaf.

No.	Retention time (min)	Compound	Molecular formula	Molecular weight	Peak area (%)	Activity	Reference
1.	10.44	alpha-Copaene	$C_{15}H_{24}$	204	3.42	Antioxidants, antigenotoxic	(Sutomo et al., 2021)
2.	16.71	Hexadecanoic acid, methyl ester	$C_{17}H_{34}O_2$	270	2.03	Antioxidant, lowers blood cholesterol, and anti-inflammatory	(Aparna et al., 2012)
3.	18.36	11-Octadecenoic acid, methyl ester	$C_{19}H_{36}O_2$	296	3.48	Antioxidant, antibacterial, antifungal, and lowers blood cholesterol	(Asghar et al., 2011)
4.	18.59	Phytol	$C_{20}H_{40}O$	296	8,13	Antihyperalgesic, anti-inflammatory, anti-arthritis, antimicrobial, and anticancer	(Carvalho et al., 2020; Willie et al., 2021)
5.	22.64	Friedelan-3-one	$C_{30}H_{50}O$	426	14.04	Antioxidant, anti-inflammatory, analgesic, antipyretic, antimicrobial, antiviral, hypolipidemic, gastroprotective, and antihyperglycemic	(Radi et al., 2023)
6.	27.07	dl-a-Tocopherol	$C_{29}H_{50}O_2$	430	8,45	Anti-inflammatory, antioxidant, and antibacterial	(Barros et al., 2020; Campoccia et al., 2015; Richard et al., 2018)
7.	30.08	Ethyl iso-allocholate	$C_{26}H_{44}O_5$	436	9.94	Anti-inflammatory, anticancer, antimicrobial, anti-asthmatic, and diuretic	(Huang et al., 2005)
8.	31.20	Lupeol	$C_{30}H_{50}O$	426	34.16	Antioxidant, anticancer, anti-inflammatory, and cardioprotective	(Dalimunthe et al., 2024; Saleem, 2009)

MDA level and catalase enzyme activity

The results of MDA level assessment are presented in **Figure 2.** The administration of seburo leaf extract and fractions at a dose of 100 mg/kgBW significantly reduced MDA levels compared to the negative control group. The mean MDA concentrations for the positive control group, n-hexane fraction, ethanol extract, ethyl acetate fraction, and ethanol-water fraction were 0.734 ± 0.087, 0.748 ± 0.061, 0.840 ± 0.068, 1.292 ± 0.050, and 1.377 ± 0.056 nmol/mL, respectively. In contrast, the negative control group exhibited a significantly higher MDA level (2.428 ± 0.075 nmol/mL) ($p < 0.05$). These findings demonstrate that treatment with seburo leaf extract and fractions effectively mitigates lipid peroxidation and reduces oxidative stress induced by CCl_4.

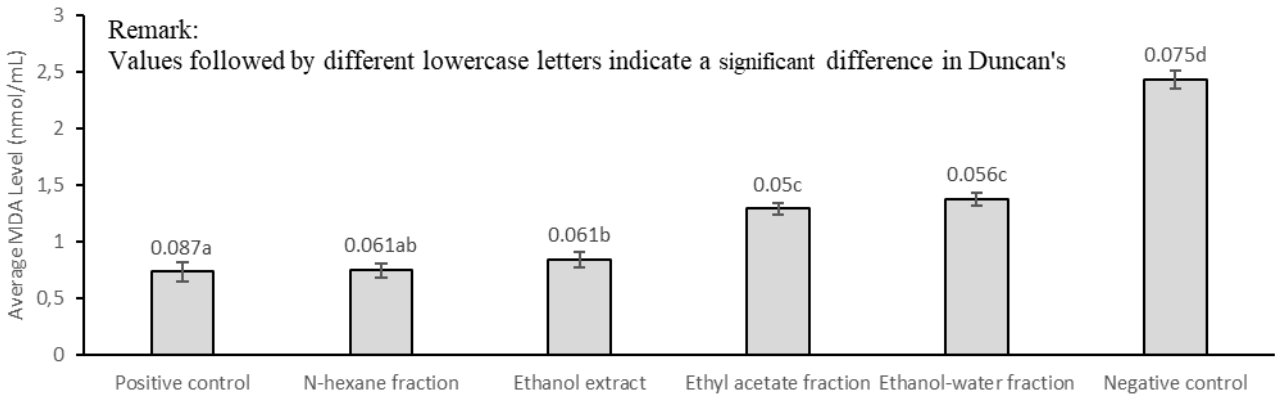

Figure 2. Average plasma MDA levels in rats.

The results of catalase enzyme measurements of rat liver tissue induced by CCl_4 are shown in **Figure 3**. The measurement results of catalase enzyme in rat liver tissue indicated an elevation in the positive control group and the treatment groups of n-hexane fraction, ethanol extract, ethyl acetate fraction, and ethanol-water fraction, with average catalase enzyme values of 29.424 ± 1.792, 27.694 ± 1.135, 26.835 ± 2.064, 21.148 ± 1.135, and 16.168 ± 0.350 U/mL, respectively. The negative control group showed lower catalase enzyme activity (10.519 ± 0.423 U/mL) compared to the positive control group and the treatment group ($p<0.05$). The results demonstrate that the treatment group that administered the extract and fraction of seburo leaves can elevate catalase enzyme levels in rat liver tissue.

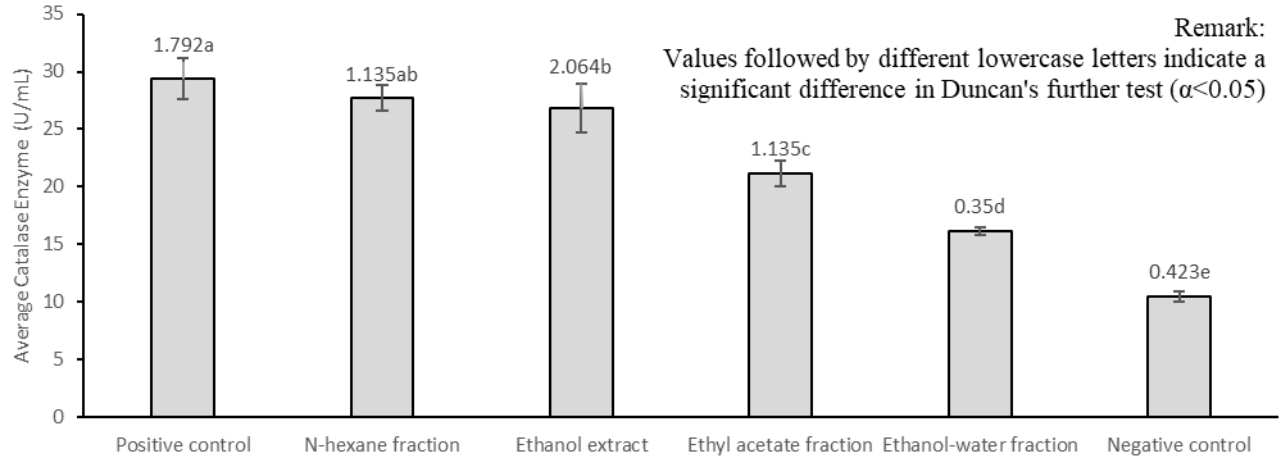

Figure 3. Average catalase enzyme in rat liver homogenate.

Macroscopic observation and histological examination of liver

Macroscopic observations made include the color and surface of the liver organ. The results of macroscopic observations of the liver can be seen in **Table 11** and **Figure 4**. Histological examination included the assessment of hydropic degeneration, fatty degeneration (Steatosis) and necrosis to determine the level of damage to liver cells (hepatocytes). The results of liver histological observations can be seen in **Table 12** and **Figure 5**.

Table 11. Results of macroscopic observation of rat liver organs.

Group	Color	Surface
Positive control	Brownish red	Smooth
Negative control	Pale red	Spots
Ethanol extract	Brownish red	Smooth
N-hexane fraction	Brownish red	Smooth
Ethyl acetate fraction	Brownish red	Smooth
Ethanol-water fraction	Brownish red	Smooth

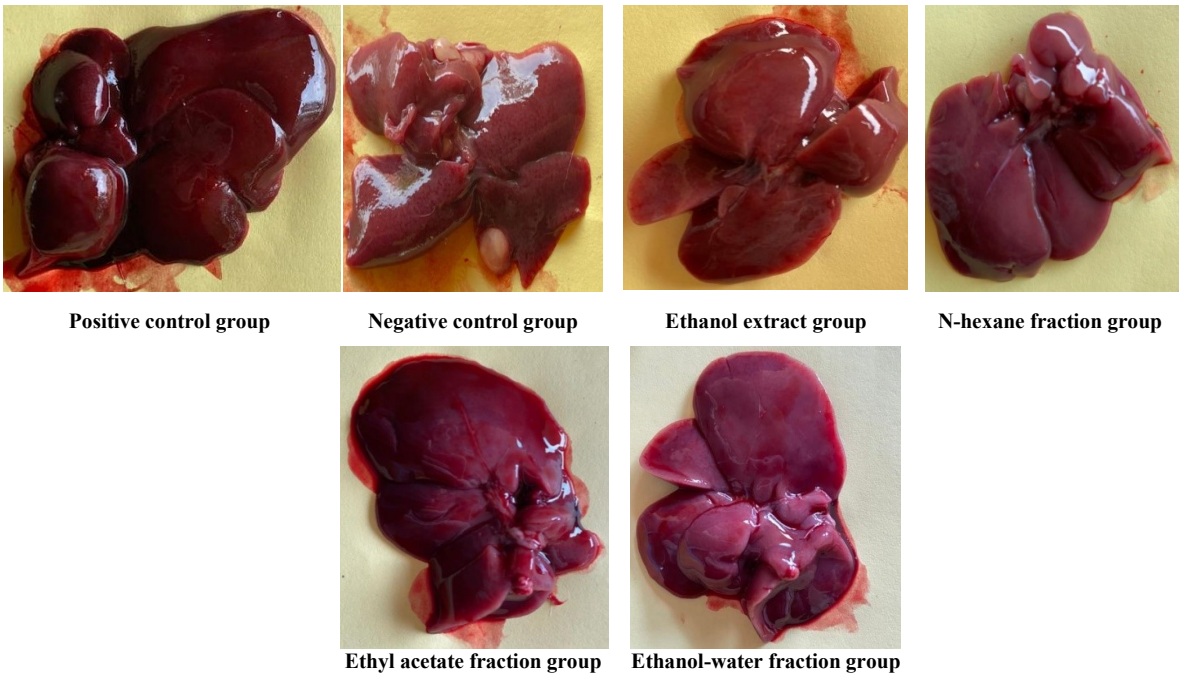

Figure 4. Macroscopic view of rat liver.

Table 12. Results of histological examination of liver tissue.

No.	Group	Hydropic degeneration	Fatty Degeneration (Steatosis)	Necrosis
1.	Positive control	0	0	0
2.	Negative control	2	3	1
3.	Ethanol extract	0	0	1
4.	N-hexane fraction	0	0	1
5.	Ethyl acetate fraction	1	0	1
6.	Ethanol-water fraction	1	0	1

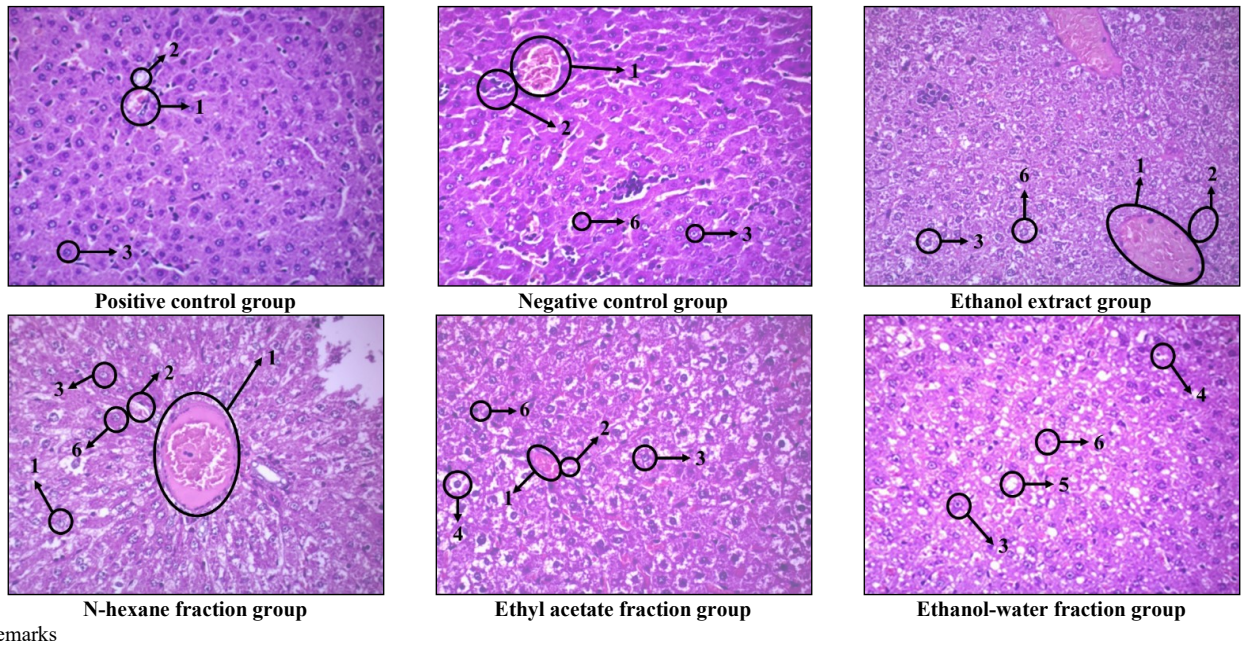

Figure 5. Histology of rat liver tissue at 40 x 10 magnification.

Discussion

The outcomes of fractionation are presented in **Table 5**. The polarity of the solvent employed in fractionation, specifically n-hexane, which possesses non-polar characteristics, effectively attracts secondary metabolites such as terpenoid, sterol, lignin, and aglycone (Widyawati et al., 2014). The semi-polar solvent ethyl acetate can effectively attract secondary metabolites, including alkaloids, steroids, aglycones, glycosides, and flavonoids (Pranata et al., 2022). The polar ethanol-water solvent can attract secondary metabolites, including phenolics, alkaloids, flavonoids, tannins and saponins (Ben et al., 2013; Gong et al., 2016).

The highest flavonoid content was shown by the ethanol extract with an amount of 33,640 ± 0.744 mg QE/g (**Table 6**). This content is comparable to the methanol extract of the stem bark of the same plant from in the study of (Wairata et al., 2022) which is 35.97 ± 0.02 mg QE/g. Meanwhile, among the fractions, ethyl acetate fraction possesses the highest concentration of flavonoids. Flavonoids can contribute to the antioxidant potential of the extract, primarily attributed to their ability to scavenge free radicals and modulate oxidative stress through several mechanisms. Certain hydroxyl groups in the flavonoid structure significantly enhance their ability to scavenge free radicals (Hou et al., 2025). Flavonoids have been shown to inhibit key oxidases, thereby preventing the generation of additional free radicals (Speisky et al., 2022). Another mechanism by which flavonoids exert their antioxidant effects is through metal chelation, in which flavonoids can bind to transition metals, preventing metal-mediated free radical generation and protecting cells from oxidative stress (Hou et al., 2025).

The highest total phenolic content was in the ethanol extract at 76.38% (**Table 7**). This level is higher than the ethanol-water extract from seburo fruit, which is 0.888% (Rizki et al., 2023). Meanwhile, among the fractions, n-hexane fraction possesses the highest concentration of phenolic content. Phenolic compounds demonstrate potent antioxidant activity through several mechanisms, including free radical scavenging via hydrogen atom donation from hydroxyl groups, metal ion chelation to inhibit Fenton-type reactions, and enhancement of endogenous antioxidant enzymes such as superoxide dismutase and catalase (Xiang et al., 2020; Yadav et al., 2023). They also protect lipids and proteins from oxidative damage, particularly by preventing lipid peroxidation, thereby maintaining cellular integrity (Xiang et al., 2020).

Thin layer chromatography (TLC) visualization using 1% H_2SO_4 was employed to classify the antioxidant compounds based on the color reactions observed. The ethanol extract was found to contain five major classes of phytochemicals: triterpenoids, steroids, phenolics, flavonoids, and tannins. Among the fractions, the n-hexane fraction showed the most diverse phytochemical profile, resembling that of the ethanol extract

Lupeol is the highest content compound in ethanol extract of *seburo* leaf (**Table 9**). Lupeol is a group of triterpene compounds which have activity as an antioxidant, anticancer, anti-inflammatory and cardioprotective (Eldohaji et al., 2021; Kapisiz et al., 2024; Malekinejad et al., 2023). Alpha copaene, phytol, Friedelan-3-one compounds are terpenoid groups. Hexadecanoic acid, methyl ester, 11-Octadecenoic acid, methyl ester, Ethyl iso-allocholate compounds are fatty acid groups. dl-a-Tocopherol compounds are lipid groups.

Lipid peroxidation refers to the oxidative degradation of polyunsaturated fatty acids in cell membranes, leading to the formation of lipid hydroperoxides and subsequent generation of malondialdehyde (MDA), a reactive aldehyde and key biomarker of oxidative stress (Cordiano et al., 2023; Wang & Zhang, 2021). MDA can covalently modify proteins, forming advanced lipoxidation and products that contribute to cellular dysfunction. The elevated MDA levels observed in the negative control group reflect extensive oxidative damage resulting from CCl_4 administration. CCl_4 is metabolized by cytochrome P450 enzymes into reactive trichloromethyl radicals, which initiate oxidative stress and can lead to liver pathologies such as cirrhosis and fibrosis (Divyashree et al., 2022).

The reduction in MDA levels is attributable to antioxidant mechanism of secondary metabolites in the extract and a fraction of *seburo* leaves. Phenolics function as free radical scavengers and metal chelators, capable of inhibiting lipid peroxidation and thus serving as antioxidants (Zeb, 2020). Triterpenoids and steroids function by diminishing the generation of new free radicals, interrupting chain reactions, and transforming them into more stable compounds (Garifullina et al., 2024). Carotenoids within triterpenoids function as antioxidants by safeguarding biological systems and mitigating damage induced by reactive oxygen species (Garifullina et al., 2024). Flavonoids function via their redox-active phenolic groups, interacting with various ROS or target molecules implicated in their generation, thereby mitigating oxidative stress or enhancing cellular metabolism (Speisky et al., 2022).

The secondary metabolites found in the extract and fractions of *seburo* leaves play a significant role in enhancing catalase enzyme activity in rat liver tissue. Beyond their intrinsic antioxidant properties, these compounds may increase catalase activity through multiple biochemical pathways. Phenolic compounds are known to directly stimulate catalase function, while triterpenoids have been reported to upregulate the expression of antioxidant enzymes, including catalase, by activating key transcription factors (Rajamanickam & Manju, 2020; Shukla et al., 2017). Additionally, flavonoids such as quercetin have been shown to interact

directly with the catalase enzyme, potentially altering its conformation and enhancing its activity through hydrophobic interactions and hydrogen bonding (Rashtbari et al., 2017). These mechanisms collectively contribute to the observed elevation in catalase activity, supporting the protective effect of *seburo* leaf constituents against oxidative stress.

A correlation study using Pearson was conducted to examine the association between plasma MDA levels and liver tissue catalase enzyme activity. The correlation results revealed a significant value of 0.000 ($p < 0.05$) and a correlation coefficient of -0.934, indicating a significant relationship between MDA levels and catalase enzyme activity; as MDA levels decrease, catalase enzyme activity increases, and vice versa.

The macroscopic examination of the liver in the positive control group revealed brownish red color with a smooth surface, devoid of spots and cysts, consistent with normal hepatic conditions. A normal liver has reddish-brown characteristics due to blood flow, but a defective liver displays surface texture alterations, including connective tissue, fatty deposits, and a lighter coloration (Fortea et al., 2018). The macroscopic examination results of the liver in the ethanol extract group, n-hexane fraction, ethyl acetate fraction, and ethanol-water fraction at a dosage of 100 mg/kgBW demonstrate the potential to mitigate the adverse effects resulting from damage induced by the hepatotoxic agent CCl_4. This is evidenced by a uniform reddish-brown liver devoid of any surface lesions, similar to standard liver conditions. Meanwhile, the negative control group exhibited a pale red liver with dots and white protrusions on its surface.

The histological examination of the liver reveals hepatocytes, the primary cellular component, organized around the major vein (**Figure 5**). Sinusoids, which are capillary blood vessels, transport blood to the central vein between the hepatocytes. Hepatocyte injury may manifest reversibly, encompassing hydropic degeneration and fatty degeneration. This damage is believed to result from elevated levels of free radicals in liver tissue following the administration of the hepatotoxic agent CCl_4. Hydropic degeneration occurs owing to cells exposed to free radical experience lipid peroxidation, undermining the integrity of the cell membrane and leading to membrane leakage (Luz et al., 2015). Fatty degeneration in the liver is characterized by the presence of empty vacuoles of varying sizes inside the liver cytoplasm. This fatty process is reversible and results from the blockage of lipid transfer release from within the cell, as well as an imbalance in the synthesis and release of triglycerides by parenchymal cells into circulation (Salguero et al., 2018). Cells experiencing necrosis exhibit features where the cell nucleus appears dark and denser (pyknotic), subsequently undergoes fragmentation into several segments (karyorrhexis), and ultimately vanishes, rendering the cell devoid of content (karyolitic) (Kroemer et al., 2009).

The positive control group administered vitamin C exhibited normal hepatocytes, with cytoplasm and nucleus free from abnormalities such as hydropic degeneration, fatty degeneration, and necrosis. The negative control subjected to CCl_4 without treatment exhibited substantial liver cell damage, characterized by hydropic degeneration, fatty degeneration, and necrosis, with respective scores of 2, 3, and 1. Histological examination of the liver in the n-hexane fraction and ethanol extract treatment groups revealed identical mild damage characterized by necrosis, assigned a score of 1. Neither treatment group exhibited hydropic degeneration or fatty degeneration. The histological examination results of the liver in the ethyl acetate and ethanol-water fraction treatment groups indicated fatty degeneration and necrosis, with a score of 1, categorizing it as mild. In comparison to the negative control group, the treatment group administered the extract and fraction of seburo leaves exhibited modest damage. The liver test results validate the biomarker findings, suggesting that the treatment of seburo leaf extract and its fractions can function as an antioxidant in rats against CCL_4.

CONCLUSIONS

The ethanol extract and fractions of *seburo* (*Garcinia forbesii King*) leaves demonstrated antioxidant activity in a CCl_4-induced hepatotoxicity model in male Wistar rats. Notably, the n-hexane fraction exhibited the most potent antioxidant activity that statistically comparable to the positive control with the lowest plasma MDA level (0.748 ± 0.061 nmol/mL), highest catalase activity (27.694 ± 1.135 U/mL), and minimal macroscopic and histological liver damage. This superior performance is likely attributable to its diverse phytochemical profile, particularly terpenoid constituents such as lupeol, α-copaene, phytol, and friedelan-3-one, which together enhance its free-radical scavenging and enzymatic antioxidant capabilities.

Acknowledgements: The author would like to express gratitude to the Genetics and Biotechnology Laboratory, Department of Biology, Faculty of Mathematics and Natural Sciences, Universitas Sriwijaya, for the research facilities provided.

Authors' Contributions: Salni designed the study. Vitri Agustiarini and Gina Nurhasana carried out the laboratory work. Gina Nurhasana analyzed the data. Salni & Vitri Agustiarini wrote the manuscript. All authors read and approved the final version of the manuscript

Competing Interests: The authors declare that there are no competing interests.

Funding: No funding.

REFERENCES

Aparna, V., Dileep, K. V., Mandal, P. K., Karthe, P., Sadasivan, C., & Haridas, M. (2012). Anti-Inflammatory Property of n -Hexadecanoic Acid: Structural Evidence and Kinetic Assessment. *Chemical Biology & Drug Design*, *80*(3), 434–439. https://doi.org/10.1111/j.1747-0285.2012.01418.x

Asghar, S. F., Habib-ur-Rehman, Choudahry, M. I., & Atta-ur-Rahman. (2011). Gas chromatography-mass spectrometry (GC-MS) analysis of petroleum ether extract (oil) and bio-assays of crude extract of Iris germanica. *International Journal of Genetics and Molecular Biology*, *3*(7), 95–100.

Aswar, A., Malik, A., Hamidu, L., & Najib, A. (2021). Determination of Total Phenolic Content of The Stem Bark Extract of Nyirih (Xylocarpus granatum J. Koeing) Using UV - Vis Spectrophotometry Method. *Jurnal Fitofarmaka Indonesia*, *8*(3), 12–17. https://doi.org/10.33096/jffi.v8i3.728

Barros, S., Ribeiro, A. P. D., Offenbacher, S., & Loewy, Z. G. (2020). Anti-inflammatory effects of vitamin e in response to candida albicans. *Microorganisms*, *8*(6), 1–13. https://doi.org/10.3390/microorganisms8060804

Ben, I. O., Woode, E., Abotsi, W. K. M., & Boakye-Gyasi, E. (2013). Preliminary Phytochemical Screening and In vitro Antioxidant Properties of Trichilia monadelpha (Thonn.). *Journal of Medical and Biomedical Sciences*, *2*(22), 6–15.

Campoccia, D., Visai, L., Renò, F., Cangini, I., Rizzi, M., Poggi, A., Montanaro, L., Rimondini, L., & Arciola, C. R. (2015). Bacterial adhesion to poly-(D,L) lactic acid blended with vitamin E: Toward gentle anti-infective biomaterials. *Journal of Biomedical Materials Research Part A*, *103*(4), 1447–1458. https://doi.org/10.1002/jbm.a.35284

Carvalho, A. M. S., Heimfarth, L., Pereira, E. W. M., Oliveira, F. S., Menezes, I. R. A., Coutinho, H. D. M., Picot, L., Antoniolli, A. R., Quintans, J. S. S., & Quintans-Júnior, L. J. (2020). Phytol, a Chlorophyll Component, Produces Antihyperalgesic, Anti-inflammatory, and Antiarthritic Effects: Possible NFκB Pathway Involvement and Reduced Levels of the Proinflammatory Cytokines TNF-α and IL-6. *Journal of Natural Products*, *83*(4), 1107–1117. https://doi.org/10.1021/acs.jnatprod.9b01116

Cordiano, R., Gioacchino, M. Di, Mangifesta, R., Panzera, C., Gangemi, S., Minciullo, P. L., & Mangifesta, C. P. 1. (2023). Structural investigation of Keap1-Nrf2 protein-protein interaction (PPI) inhibitors for treating myocarditis through molecular simulations. *New Journal of Chemistry*, *47*(18), 8524–8537. https://doi.org/10.1039/d2nj03078k

Dalimunthe, A., Carensia Gunawan, M., Dhiya Utari, Z., Dinata, M. R., Halim, P., Estherina S. Pakpahan, N., Sitohang, A. I., Sukarno, M. A., Yuandani, Harahap, Y., Setyowati, E. P., Park, M. N., Yusoff, S. D., Zainalabidin, S., Prananda, A. T., Mahadi, M. K., Kim, B., Harahap, U., & Syahputra, R. A. (2024). In-depth analysis of lupeol: delving into the diverse pharmacological profile. *Frontiers in Pharmacology*, *15*(November), 1–32. https://doi.org/10.3389/fphar.2024.1461478

Departemen Kesehatan RI. (2000). *Parameter Standar Umum Ekstrak Tumbuhan Obat*. Departemen Kesehatan.

Desmawati, D., Nisa, R., & Afriani, N. (2022). Effect of High Fat Diet on Histopathological Appearance of Pregnant Wistar Rat's Liver. *Majalah Kedokteran Bandung*, *54*(3), 148–153. https://doi.org/10.15395/mkb.v54n3.2650

Divyashree, J., Tomar, S., & Singh, A. P. (2022). Hepatoprotective action of vegetables. *International Journal of Health Sciences*, *6*(March), 9571–9576. https://doi.org/10.53730/ijhs.v6ns2.7507

Eldohaji, L. M., Fayed, B., Hamoda, A. M., Ershaid, M., Abdin, S., Alhamidi, T. B., Mohammad, M. G., Omar, H. A., & Soliman, S. S. M. (2021). Potential targeting of Hep3B liver cancer cells by lupeol isolated from Avicennia marina. *Archiv Der Pharmazie*, *354*(9). https://doi.org/10.1002/ardp.202100120

Flieger, J., Flieger, W., & Baj, J. (2021). Antioxidants : Classification , Natural Sources , Activity / Capacity. *Materials*, *14*(4135), 1–54. https://www.mdpi.com/journal/materials

Fortea, J. I., Fernández-Mena, C., Puerto, M., Ripoll, C., Almagro, J., Bañares, J., Bellón, J. M., Bañares, R., & Vaquero, J. (2018). Comparison of Two Protocols of Carbon Tetrachloride-Induced Cirrhosis in Rats – Improving Yield and Reproducibility. *Scientific Reports*, *8*(1), 9163. https://doi.org/10.1038/s41598-018-27427-9

Garifullina, G. G., Nasretdinova, R. N., Gerchikov, A. Y., Shaymordanova, G. M., Petrova, A. V., & Mustafin, A. G. (2024). Antioxidant efficiency of triterpenoids in radical chain oxidation of organic compounds. *Reaction Kinetics, Mechanisms and Catalysis*, *137*(1), 39–51. https://doi.org/10.1007/s11144-023-02516-7

Gong, J., Huang, J., Xiao, G., Chen, F., Lee, B., Ge, Q., You, Y., Liu, S., & Zhang, Y. (2016). Antioxidant capacities of fractions of bamboo shaving extract and their antioxidant components. *Molecules*, *21*(8), 1–14. https://doi.org/10.3390/molecules21080996

Haris, M. A. M., & Sani, S. A. (2022). Antioxidant screening of Garcinia Forbesii originated from Sabah. *Journal of Physics: Conference Series*, *2314*(1). https://doi.org/10.1088/1742-6596/2314/1/012031

Hidayati, F., Y.S. Darmanto, Y. S. D., & Romadhon, R. (2017). The Effect of Different Concentrations Extract Sargassum sp. and Storage Time of Lipid Oxidation at Catfish (Pangasiu). *SAINTEK PERIKANAN : Indonesian Journal of Fisheries Science and Technology*, *12*(2), 116. https://doi.org/10.14710/ijfst.12.2.116-123

Hou, Y., Wang, Y., Tan, X., Wang, Y., Li, W., & Li, X. (2025). Investigating the Antioxidant Efficiency of Tea Flavonoid Derivatives: A Density Functional Theory Study. *International Journal of Molecular Sciences*, *26*(6), 1–14. https://doi.org/10.3390/ijms26062587

Huang, D., Ou, B., & Prior, R. L. (2005). The Chemistry behind Antioxidant Capacity Assays. *Journal of Agricultural and Food Chemistry*, *53*(6), 1841–1856. https://doi.org/10.1021/jf030723c

Kapisiz, A., Kaya, C., Eryilmaz, S., Karabulut, R., Turkyilmaz, Z., Inan, M., Gulbahar, O., & Sonmez, K. (2024). Protective effects of lupeol in rats with renal ischemia-reperfusion injury. *Experimental and Therapeutic Medicine*, *28*(2), 313. https://doi.org/10.3892/etm.2024.12602

Kornienko, J. S., Smirnova, I. S., Pugovkina, N. A., Ivanova, J. S., Shilina, M. A., Grinchuk, T. M., Shatrova, A. N., Aksenov, N. D., Zenin, V. V., Nikolsky, N. N., & Lyublinskaya, O. G. (2019). High doses of synthetic antioxidants induce premature senescence in cultivated mesenchymal stem cells. *Scientific Reports*, *9*(1), 1–13. https://doi.org/10.1038/s41598-018-37972-y

Kroemer, G., Galluzzi, L., Vandenabeele, P., Abrams, J., Alnemri, E. S., Baehrecke, E. H., Blagosklonny, M. V., El-Deiry, W. S., Golstein, P., Green, D. R., Hengartner, M., Knight, R. A., Kumar, S., Lipton, S. A., Malorni, W., Nuñez, G., Peter, M. E.,

Tschopp, J., Yuan, J., … Melino, G. (2009). Classification of cell death: Recommendations of the Nomenclature Committee on Cell Death 2009. *Cell Death and Differentiation*, *16*(1), 3–11. https://doi.org/10.1038/cdd.2008.150

Luz, S. C. A. Da, Daubermann, M. F., Thomé, G. R., dos Santos, M. M., Ramos, A., Torres Salazar, G., da Rocha, J. B. T., & Barbosa, N. V. (2015). Diphenyl Ditelluride Intoxication Triggers Histological Changes in Liver, Kidney, and Lung of Mice. *Analytical Cellular Pathology*, *2015*, 1–10. https://doi.org/10.1155/2015/784612

Malekinejad, H., Zeynali-Moghaddam, S., Rezaei-Golmisheh, A., Alenabi, A., Malekinejad, F., Alizadeh, A., & Shafie-Irannejad, V. (2023). Lupeol attenuated the NAFLD and PCOS-induced metabolic, oxidative, hormonal, histopathological, and molecular injuries in mice. *Research in Pharmaceutical Sciences*, *18*(5), 551–565. https://doi.org/10.4103/1735-5362.383710

Muthia, R., Saputri, R., & Verawati, S. A. (2019). Uji Aktivitas Antioksidan Ekstrak Etanol Kulit Buah Mundar (Garcinia forbesii King.) Menggunakan Metode DPPH (2,2-Diphenyl-1-Picrylhydrazil). *Jurnal Pharmascience*, *6*(1), 74. https://doi.org/10.20527/jps.v6i1.6079

Pranata, A., Tutik, T., & Marcellia, S. (2022). Perbandingan Efektivitas Ekstrak Etil Asetat dan N-Heksana Kulit Bawang Merah (Allium cepa L.) SEBAGAI LARVASIDA Aedes aegypti. *Jurnal Ilmu Kedokteran Dan Kesehatan*, *8*(4), 325–333. https://doi.org/10.33024/jikk.v8i4.5140

Purkon, D. B., Kusmiyati, M., Trinovani, E., Fadhlillah, F. M., Widyastiwi, W., Roseno, M. H., Khristian, E., & Nadhifah, A. (2022). The hepatoprotective effect of Marchantia paleacea bertol. extract against acetaminophen-induced liver damage in rat: biochemical and histological evidence. *Journal of Research in Pharmacy*, *26*(6), 1857–1867. https://doi.org/10.29228/jrp.275

Radi, M. H., El-Shiekh, R. A., El-Halawany, A. M., & Abdel-Sattar, E. (2023). Friedelin and 3β-Friedelinol: Pharmacological Activities. *Revista Brasileira de Farmacognosia*, *33*(5), 886–900. https://doi.org/10.1007/s43450-023-00415-5

Rahma, K., & Purnomo, F. O. (2023). Potential Effects of Ipomoea reptans Poir. Extract on LDL, HDL levels and liver Histopathology. *Journal of Biomedicine and Translational Research*, *9*(2), 61–67. https://doi.org/10.14710/jbtr.v9i2.16984

Rajamanickam, G., & Manju, S. . (2020). Identification and Comparative Study of Invitro Antioxidant Potential of Fractionated Hydroalcoholic Extract of Phyllanthus Niruri Linn. *European Journal of Advanced Chemistry Research*, *1*(1), 1–8. https://doi.org/10.24018/ejchem.2020.1.1.2

Rashtbari, S., Dehghan, G., Yekta, R., & Jouyban, A. (2017). Investigation of the binding mechanism and inhibition of bovine liver catalase by quercetin: Multi-spectroscopic and computational study. *BioImpacts*, *7*(3), 147–153. https://doi.org/10.15171/bi.2017.18

Richard, E. L., Laughlin, G. A., Kritz-Silverstein, D., Reas, E. T., Barrett-Connor, E., & McEvoy, L. K. (2018). Dietary patterns and cognitive function among older community-dwelling adults. *Nutrients*, *10*(8), 1–15. https://doi.org/10.3390/nu10081088

Rizki, M. I., Triyasmono, L., Alfandi, G., Akbar, N. H., & Sari, A. K. (2023). Characterization of mundar pericarp (Garcinia forbesii) extract from banjar district of Indonesia. *Jurnal Insan Farmasi Indonesia*, *6*(2), 232–241. https://doi.org/10.36387/jifi.v6i2.1589

Saleem, M. (2009). Lupeol, a novel anti-inflammatory and anti-cancer dietary triterpene. *Cancer Letters*, *285*(2), 109–115. https://doi.org/10.1016/j.canlet.2009.04.033

Salguero, F. J., Garcia-Jimenez, W. L., Lima, I., & Seifert, K. (2018). Histopathological and immunohistochemical characterisation of hepatic granulomas in Leishmania donovani-infected BALB/c mice: A time-course study. *Parasites and Vectors*, *11*(1), 1–9. https://doi.org/10.1186/s13071-018-2624-z

Shukla, K., Pal, P. B., Sonowal, H., Srivastava, S. K., & Ramana, K. V. (2017). Aldose Reductase Inhibitor Protects against Hyperglycemic Stress by Activating Nrf2-Dependent Antioxidant Proteins. *Journal of Diabetes Research*, *2017*, 1–9. https://doi.org/10.1155/2017/6785852

Speisky, H., Shahidi, F., de Camargo, A. C., & Fuentes, J. (2022). Revisiting the Oxidation of Flavonoids: Loss, Conservation or Enhancement of Their Antioxidant Properties. *Antioxidants*, *11*(1), 1–28. https://doi.org/10.3390/antiox11010133

Sutomo, Kiptiah, M., Nurmaidah, & Arnida. (2021). Identifikasi Potensi Senyawa Antioksidan Dari Fraksi Etil Asetat Dsun Mundar (*Garcinia forbesii* King .) Asal Kalimantan Selatan. *Prosiding Seminar Nasional Lingkungan Lahan Basah*, *6*(3), 6.

Sutomo, S., Kamali, D. N., Arnida, A., Normaidah, N., & Sriyono, A. (2020). Pharmacognostic Study and Antioxidant Activity of Mundar (Garcinia forbesii King.) leaves from Banua Botanical Gardens of South Kalimantan. *Borneo Journal of Pharmacy*, *3*(4), 209–215. https://doi.org/10.33084/bjop.v3i4.1541

To, A., N, N., & Co, N. (2020). Identification of Potential Antioxidant and Hepatoprotective Constituents of Vitex Doniana By Uhplc/+Esi-Qqtof-Ms/Ms Analysis. *Asian Journal of Pharmaceutical and Clinical Research*, *November*, 142–148. https://doi.org/10.22159/ajpcr.2020.v13i8.37956

Tsikas, D. (2017). Assessment of lipid peroxidation by measuring malondialdehyde (MDA) and relatives in biological samples: Analytical and biological challenges. *Analytical Biochemistry*, *524*, 13–30. https://doi.org/10.1016/j.ab.2016.10.021

Wairata, J., Fadlan, A., Setyo Purnomo, A., Taher, M., & Ersam, T. (2022). Total phenolic and flavonoid contents, antioxidant, antidiabetic and antiplasmodial activities of Garcinia forbesii King: A correlation study. *Arabian Journal of Chemistry*, *15*(2), 103541. https://doi.org/10.1016/j.arabjc.2021.103541

Wairata, J., Sukandar, E. R., Fadlan, A., Purnomo, A. S., Taher, M., & Ersam, T. (2021). Evaluation of the antioxidant, antidiabetic, and antiplasmodial activities of xanthones isolated from garcinia forbesii and their in silico studies. *Biomedicines*, *9*(10). https://doi.org/10.3390/biomedicines9101380

Wang, J., & Zhang, X. (2021). Free-Radical-Initiated Phospholipid Oxidations at the Air–Water Interface: The Oxidation of Unsaturated and Saturated Fatty Acid Chains. *The Journal of Physical Chemistry A*, *125*(4), 973–979. https://doi.org/10.1021/acs.jpca.0c10170

Wathan, N., Rizki, M. I., Khairunnisa, A., & Simamora, H. (2023). Total Flavonoids Determination and Antioxidant Activity of Ethyl Acetate, Ethanol, and Methanol Extracts from Seluang Belum Root (Luvunga sarmentosa (Blume) Kurz.). *Berkala Kedokteran*, *19*(1), 101. https://doi.org/10.20527/jbk.v19i1.15733

Widiyana, A. P., & Illian, D. N. (2022). Phytochemical Analysis and Total Flavonoid Content on Ethanol and Ethyl Acetate Extract From Neem (Azadirachta Indica Juss.) Leaves Utilizing Uv–Vis Spectrophotometric. *Jurnal Farmasi Sains Dan Praktis*, *8*(1), 71–77. https://doi.org/10.31603/pharmacy.v8i1.6582

Widyawati, P. S., Budianta, T. D. W., Kusuma, F. A., & Wijaya, E. L. (2014). Difference of solvent polarity to phytochemical content and antioxidant activity of Pluchea indicia less leaves extracts. *International Journal of Pharmacognosy and Phytochemical Research*, *6*(4), 850–855.

Willie, P., Uyoh, E. A., & Aikpokpodion, P. O. (2021). Gas chromatography-mass spectrometry (GC-MS) assay of bio-active compounds and phytochemical analyses in three species of apocynaceae. *Pharmacognosy Journal*, *13*(2), 383–392. https://doi.org/10.5530/pj.2021.13.49

Wulandari, L., Dewi, M. K. C., Kristiningrum, N., & Siswanti, R. A. Y. N. (2020). Determination of total phenolic content and nir-chemometrics classification model of queen and local varieties of soursop (*Annonamuricata l.*) leaf powder. *Indonesian Journal of Chemistry*, *20*(3), 520–529. https://doi.org/10.22146/ijc.43051

Xiang, Z., Wu, X., Liu, X., & Chen, G. (2020). Antioxidant phenolic compounds from chinese white olive (canarium album l.). *Bangladesh Journal of Botany*, *49*(4), 1029–1035. https://doi.org/10.3329/bjb.v49i4.52535

Yadav, P., Chaudhary, P., Kumari, D., & Janmeda, P. (2023). Assessment of phytochemical screening and antioxidant potential of Heteropogon contortus (L.) whole plant. *The Applied Biology & Chemistry Journal*, *3*(2022), 62–70. https://doi.org/10.52679/tabcj.2022.0007

Zeb, A. (2020). Concept, mechanism, and applications of phenolic antioxidants in foods. *Journal of Food Biochemistry*, *44*(9). https://doi.org/10.1111/jfbc.13394

Zega, A. M., Tandanu, E., & Wardhani, F. M. (2023). Toxicity Test of White Turmeric (*Curcuma Zedoaria*) on Liver Organs in White Male Rats. *Jurnal Kedokteran Raflesia*, *7*(1), 51–58. https://doi.org/10.33369/juke.v7i1.19102